FREQUENCY AGILE PMUT-BASED ULTRASONIC COMMUNICATION LINKS

Bernard Herrera[1], *Flavius Pop*[1], *Cristian Cassella*[1], *and Matteo Rinaldi*[1]
[1]Northeastern SMART Center, Northeastern University, Boston, USA

ABSTRACT

The present work reports on the generation of distinct ultrasonic communication frequency bands by using a single Piezoelectric Micro-Machined Ultrasonic Transducer (PMUT) array. In contrast to the common use of these transducers within their resonance band, off-band operation is enabled through the use of specially designed broadband matching networks. By harnessing the capacitive nature of a fabricated PMUT array and its good matching with the medium, transmission improvements of up to 15 dB over 0.2 fractional bandwidths around 2 and 3 MHz center frequencies were achieved on a transducer resonating at 1.1 MHz. The resulting sharp roll-off and good off-band rejection for the acoustic channels are crucial features for the implementation of intra-body networks with multiple, simultaneously transmitting nodes with different bandwidth requirements (fig. 1).

INTRODUCTION

The use of PMUTs in applications such as ultrasound imaging [1] or range-finding [2], has been widely investigated and even commercial technologies have been developed around PMUT arrays as transducers for fingerprint scanning [3]. Several works, focused on device level improvements, have also increased the transducer bandwidth in water by the merging of resonant modes [4], [5], [6]. However, the use of PMUT arrays as transmitters and receivers on acoustic communication channels has not been widely explored.

On the other hand, the promising potential of ultrasonic wireless communication for intra-body networks has been demonstrated using commercially available Lead Zirconium Titanate (PZT) ultrasonic transducers [7]. Furthermore, ultrasonic network flexibility has been addressed in an underwater communication context [8], [9].

The present work brings together these efforts by introducing PMUTs as transceivers and demonstrating an effective scheme for improving their performance over broad frequency bands that can be arbitrarily designed. This further enables the devices for intra-body networking applications implementing more complex communication schemes.

Beyond that, the particular choice of Aluminum Nitride (AlN) PMUTs as transducers proves advantageous due to their superior acoustic medium matching, capability of chip integration with Complementary Metal Oxide Semiconductor (CMOS) technologies, miniaturized dimensions and bio-compatibility of AlN as a piezoelectric as compared to PZT-based transducers.

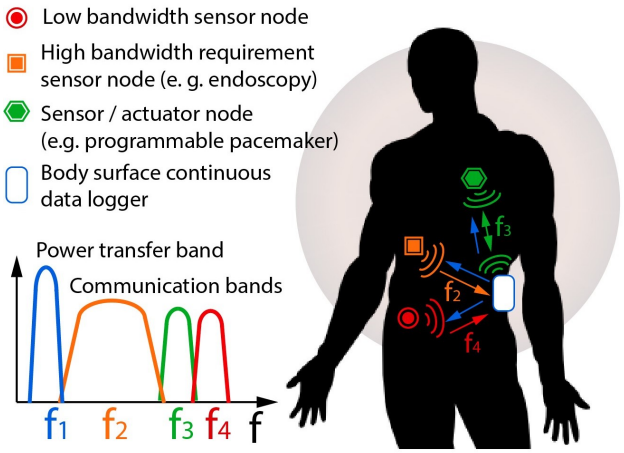

Figure 1: Envisioned multi-node intra-body network. *Matching networks coupled to the transducers of the sensing nodes and an external data logger enable spectral flexibility and interference rejection from other nodes.*

METHODOLOGY

20 x 20 element rectangular arrays of Aluminum Nitride (AlN) PMUTs were fabricated to be used as the ultrasonic transmitter element of the acoustic communication link (fig. 3). The medium of choice for the transmission was dielectric oil, as it closely emulates the characteristics of the desired intra-body medium while having a low conductivity that reduces transmission of signals that are not exclusively acoustic.

The admittance of the transducers was measured while submerged in the dielectric oil and, from this measurement, their static capacitance value (C_0) was obtained. Based on C_0, and the desired center frequency and bandwidth of operation of the communication link, a third order LC Chebyshev band-pass filter was designed where the series capacitor, C_s, of the filter circuit was replaced with the PMUT array (fig. 2). The reasoning behind the approach is that, due to the capacitive nature of the transducer, its static capacitance acts as a part of the filter, setting the passband while benefitting from a voltage gain due to impedance matching.

For a third order Chebyshev bandpass filter with a 0.1 dB ripple, the design equations are:

$$C_s = \frac{B}{2\pi f_0 Z_0 g_1} \tag{1}$$

$$L_p = \frac{B Z_0}{2\pi f_0 g_2} \tag{2}$$

$$C_p = \frac{g_2}{2\pi f_0 Z_0 B} \tag{3}$$

$$L_s = \frac{Z_0 g_1}{2\pi f_0 B} \tag{4}$$

where L_p, L_s, C_s and C_p are the values of the passive components used in the filter, f_0 is the center frequency of the passband, B is the fractional bandwidth, Z_0 is the characteristic impedance and $g_1 = 1.03156$ and $g_2 = 1.1474$ are the filter prototype coefficients.

It can be seen that, once the desired center frequency, characteristic impedance and C_s are set, the rest of the parameters can be calculated to define the complete circuit. To match with standard communication equipment, Z_0 is set to 50 Ω. C_s can then be made equal to the measured C_0 of the transducer which sets the last remaining variable, B.

Tuning is required on the values of the passive components after the calculation of their design values to account for only standard values being available and to limited quality factors (Q) for inductors at the relatively low frequencies of operation for the ultrasonic links. The tuning process was performed using a circuit simulator with the measured S-parameter file for the PMUT array.

Even though, B is set for a specific transducer and desired frequency of operation, if a larger bandwidth is desired, C_s can be calculated as a dependent variable for a defined B. Transmission gain on the passband can still be attained empirically in this case, after tuning the parameters of the circuit to account for the mismatch.

The particular transducer used in this work has a resonant frequency of 1.1 MHz when operated in fluid. Matching networks were designed around 2 MHz and 3 MHz with fractional bandwidths of 0.2 and 0.5 to showcase the frequency flexibility of the approach. The simulated voltage gain seen at the input of the PMUT array as compared to operation without matching circuits can be seen to the left of fig. 4.

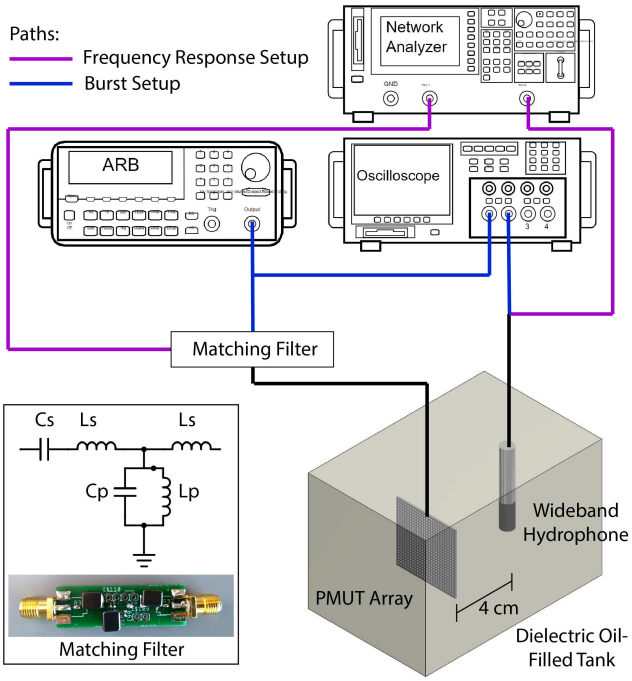

Figure 2: Schematic of the measurement setup. *Both connections for frequency response and burst measurements are shown. The PMUT array's static capacitance C_0 replaces the second series capacitance C_s of the Chebyshev filter*

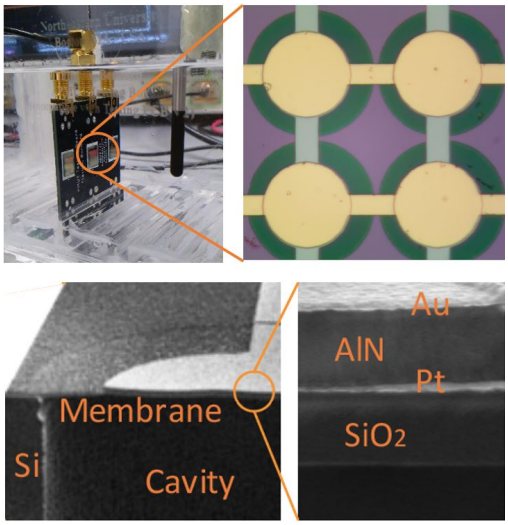

Figure 3: Optical (top) and Scanning Electron Microscope (bottom) images of fabricated PMUT Array.

The particular choice of frequencies of operation responds to the fact that attenuation in the aqueous medium increases with frequency, so relatively low operating values are preferred. However, any arbitrary center frequency could have been chosen.

FABRICATION

The AlN PMUTs were fabricated on a silicon wafer using a 4 masks microfabrication process. A double-side polished, 300 μm silicon wafer was used as a substrate. An 850 nm silicon dioxide layer was then deposited through Plasma Enhanced Chemical Vapor Deposition (PECVD). A 5 nm Pt / 95 nm Ti bottom electrode was then formed by electron beam evaporation and patterned through a photo lithography and liftoff process. 800 nm of the piezoelectric AlN were then reactively sputtered and vias were etched through the layer for access to the bottom electrode by hot phosphoric acid etching. The material stack was completed with a sputtered 5nm Ti / 50nm Au top electrode. Back-side alignment photolithography and Deep Reactive Ion Etching (DRIE) were finally used to etch cavities and release the device membrane (fig. 3).

RESULTS

Transmission gain improvement and bandwidth of operation were experimentally verified by two measurement setups (fig. 2) one characterizing the frequency domain response of the system and other its time domain response.

A Vector Network Analyzer (VNA) measured the transmission frequency response from the PMUT array, through a dielectric oil medium and to a wideband reference hydrophone . The baseline response, without matching, showed a resonant band at 1.1 MHz and a second mode at 2.5 MHz. The responses when connecting 2 MHz and 3 MHz matching filters showed 10-15 dB higher transmission values over the designed bands. For very large bandwidths (0.5 for 2 MHz filter 2) ripples in the filter result in high gain but a less flat response (fig. 4, left).

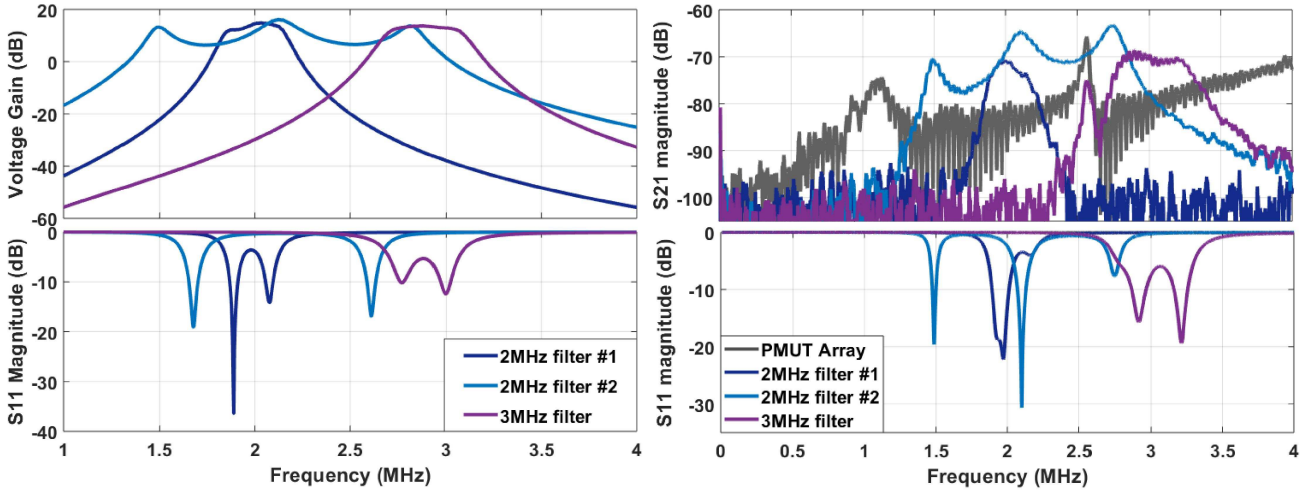

Figure 4: Simulated and measured performance of communication links with matching networks. *Left: Simulated PMUT voltage gain and matching network input reflection coefficient magnitude for three representative designed matching networks. Right: Vector network analyzer (VNA) measured transmission (S21) and input reflection coefficient (S11) for the implemented matching networks. Note the transmission band at around 1.1 MHz and at the second mode at 2.5 MHz for the PMUT array base response. Good agreement is obtained with simulation except for a gradual increase in response with higher frequencies due to increasing capacitive coupling.*

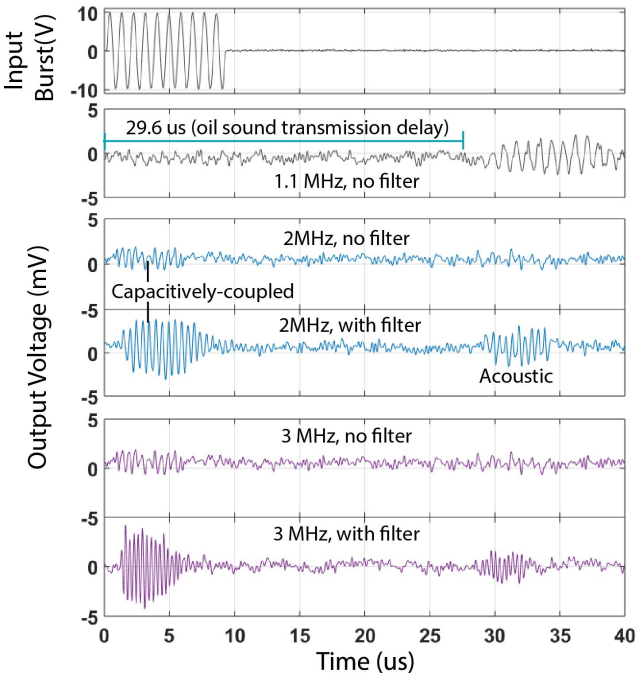

Figure 5: Responses to 10-cycle input sinusoidal burst at different frequencies. *The acoustic response can be identified as it appears with a delay corresponding to the propagation of sound in the medium at the set distance. Capacitive coupling appears simultaneously with the burst. A marked improvement in signal to noise ratio can be seen when the matching filters are used.*

Good agreement with the simulated behaviour was obtained in terms of center frequency, bandwidth and reflection coefficient S_{11}. The predicted voltage gain translates in a comparable improvement in transmission (S_{21}). It is important to note that this improvement is implemented on the full chain from the transmitter, through the medium and to the receiver, so the gain and filtering is transferred to the acoustic domain.

In the second setup, a waveform generator produced a sinusoidal burst which was applied to the transducer. A delayed acoustic response (due to sound propagation in the medium at the set distance) was observed which was 3 times larger than without matching at the same frequency, where the received signal was barely above the noise level (fig. 5).

A capacitively-coupled signal appears simultaneously with the burst due to the device not being packaged and electrically isolated and limited distance to the receiver, and it also benefits from the gain coming from the improved matching through the use of the circuits.

Results are shown for the gain of the array used as a transmitter, but the matching networks were also proven to increase sensitivity when using a PMUT array as the receiver.

CONCLUSIONS

The approach of effectively operating a PMUT array out of its resonant band by the use of custom broadband matching networks was demonstrated in the current work. Design equations based on modified pass-band Chebyshev filters and circuit simulation and tuning with the transducers S-parameters allowed to achieve transmission bands around 2 and 3 MHz, with 0.2 and 0.5 fractional bandwidths using a transducer with a resonant frequency of 1.1 MHz. The predicted gain was verified by VNA transmission measurements characterizing the frequency response of the whole communication link including the medium and through burst measurements characterizing its time response.

The technique effectively implements filtering on the acoustic domain, with good band-to-band rejection and

sharp roll-off. This allows for frequency agility in ultrasonic communication links valuable for achieving spectral efficiency in intra-body and underwater acoustic channels.

ACKNOWLEDGEMENTS

This work was supported by the NSF programs MRI-SEANet (NSF Number 1726512) and NeTS-Small (NSF Number 1618731).

The authors would like to thank the staff of the George J. Kostas Nanoscale Technology and Manufacturing Research Center for assistance in device fabrication.

REFERENCES

[1] Y. Lu, H. Tang, S. Fung, B. Boser, and D. A. Horsley, "Pulse-echo ultrasound imaging using an aln piezoelectric micromachined ultrasonic transducer array with transmit beam-forming," *Journal of Microelectromechanical Systems*, vol. 25, no. 1, pp. 179–187, 2016.

[2] Z. Zhou, S. Yoshida, and S. Tanaka, "Epitaxial pmnn-pzt/si mems ultrasonic rangefinder with 2 m rangeat 1 v drive," *Sensors and Actuators A*, vol. 266, pp. 352–360, 2017.

[3] Y. Lu, H. Tang, S. Fung, Q. Wang, J. M. Tsai, M. Daneman, B. E. Boser, and D. A. Horsley, "Ultrasonic fingerprint sensor using a piezoelectric micromachined ultrasonic transducer array integrated with complementary metal oxide semiconductor electronics," *Applied Physics Letters*, vol. 106, no. 26, p. 263503, 2015.

[4] Y. Lu, O. Rozen, H.-Y. Tang, G. L. Smith, S. Fung, B. E. Boser, R. G. Polcawich, and D. A. Horsley, "Broadband piezoelectric micromachined ultrasonic transducers based on dual resonance modes," in *Micro Electro Mechanical Systems (MEMS), 2015 28th IEEE International Conference on*, pp. 146–149, IEEE, 2015.

[5] B. E. Eovino, S. Akhbari, and L. Lin, "Broadband ring-shaped pmuts based on an acoustically induced resonance," in *Micro Electro Mechanical Systems (MEMS), 2017 IEEE 30th International Conference on*, pp. 1184–1187, IEEE, 2017.

[6] T. Wang, T. Kobayashi, and C. Lee, "Micromachined piezoelectric ultrasonic transducer with ultra-wide frequency bandwidth," *Applied Physics Letters*, vol. 106, no. 1, p. 013501, 2015.

[7] G. E. Santagati and T. Melodia, "Experimental evaluation of impulsive ultrasonic intra-body communications for implantable biomedical devices," *IEEE Transactions on Mobile Computing*, vol. 16, no. 2, pp. 367–380, 2017.

[8] E. Demirors, B. Shankar, E. Santagati, and T. Melodia, "SEANet: A Software-Defined Acoustic Networking Framework for Reconfigurable Underwater Networking," in *Proceedings of the 10th International Conference on Underwater Networks Systems*, vol. 53, p. 11, 2015.

[9] E. Demirors and T. Melodia, "Chirp-based lpd/lpi underwater acoustic communications with code-time-frequency multidimensional spreading," in *Proceedings of the 11th ACM International Conference on Underwater Networks & Systems*, p. 9, ACM, 2016.

CONTACT

Bernard Herrera Soukup; herrerasoukup.b@northeastern.edu